



Low-temperature magnetic and electrical transport properties of some ternary Ce–Rh–Si compounds

D. Kaczorowski^{a,*}, A. Lipatov^b, A. Gribanov^c, Yu. Seropegin^c

^a Institute of Low Temperature and Structure Research, Polish Academy of Sciences, P.O. Box 1410, 50-950 Wrocław, Poland

^b Department of Materials Science, Moscow State University, GSP-1, 119991 Moscow, Russia

^c Department of Chemistry, Moscow State University, GSP-1, 119991 Moscow, Russia

ARTICLE INFO

Article history:

Received 1 March 2011

Accepted 23 March 2011

Available online 1 April 2011

Keywords:

Cerium intermetallics

Magnetic behavior

Electrical resistivity

ABSTRACT

Five novel cerium-based ternaries $\text{Ce}_2\text{Rh}_{3.1}\text{Si}_{0.9}$, $\text{Ce}_4\text{Rh}_{12}\text{Si}$, $\text{Ce}_8\text{Rh}_{21.9}\text{Si}_{3.1}$, $\text{CeRh}_{1.82}\text{Si}_{0.18}$ and $\text{CeRh}_3\text{Si}_{0.125}$ were studied by means of magnetic susceptibility and electrical resistivity measurements. All these phases were found to be Pauli paramagnets with metallic type of electrical conductivity.

© 2011 Elsevier B.V. All rights reserved.

1. Introduction

The Ce–Rh–Si system is known to be exceptionally rich in ternary phases. Recently, as many as 14 novel compounds have been identified, in addition to 13 previously reported ternaries [1]. Phase equilibria in this system are characterized by significant mutual solubilities between cerium silicides and cerium–rhodium compounds, as well as by extended homogeneity regions of some of the ternaries. These two effects seem most clearly observed at 33 at.% of cerium. It has been shown in Ref. [1] that up to 6.5 at.% of Si can substitute Rh in the binary compound CeRh_2 , hence forming $\text{Ce}(\text{Rh}_{1-x}\text{Si}_x)_2$ phases. With further substitution along the line one obtains ternary compounds $\text{Ce}_{33.3}\text{Rh}_{58.2-55.2}\text{Si}_{8.5-11.5}$ (unknown structure type), $\text{Ce}_2\text{Rh}_{3+x}\text{Si}_{1-x}$ ($0.08 \leq x \leq 0.17$; $\text{Y}_2\text{Rh}_3\text{Ge}$ -type) and $\text{Ce}_2\text{Rh}_{1-x}\text{Si}_{3+x}$ ($0 \leq x \leq 0.24$; Er_2RhSi_3 -type), each with its specific homogeneity region. Finally, the formation of pseudobinary phases $\text{Ce}(\text{Rh}_x\text{Si}_{1-x})_2$ is observed with up to 10 at.% of Rh substituted for Si in the binary compound CeSi_2 . Also the region with ~25 at.% of Ce atoms exhibits similar phase formation phenomena. Here, adding Si to the binary compound CeRh_3 results in two new compounds: $\text{Ce}_4(\text{Rh}_{1-x}\text{Si}_x)_{12}\text{Si}$ ($0.00 \leq x \leq 0.03$; self-type) and $\text{Ce}_8(\text{Rh}_{1-x}\text{Si}_x)_{24}\text{Si}$ ($0.07 \leq x \leq 0.10$; $\text{Ce}_8\text{Pd}_{24}\text{Sb}$ -type). Moreover, one observes three other ternaries $\text{CeRh}_{2-x}\text{Si}_{1+x}$ ($0.0 \leq x \leq 0.1$; CeIr_2Si -type), $\text{CeRh}_{1.88}\text{Si}_{1.12}$ (inversed CeNiSi_2 -type) and $\text{Ce}_2\text{Rh}_{3-x}\text{Si}_{3+x}$

($0.05 \leq x \leq 0.36$; $\text{Ce}_2\text{Rh}_{1.35}\text{Ge}_{4.65}$ -type), and eventually the phase $\text{CeRh}_{1-x}\text{Si}_{2+x}$ ($0 \leq x \leq 0.32$; CeNiSi_2 -type).

Several ternary Ce–Rh–Si compounds have been investigated for their physical properties, and recently such studies have additionally been motivated the spectacular findings of heavy-fermion superconductivity in antiferromagnetic CeRh_2Si_2 [2] and CeRhSi_3 [3]. Though no other superconductors have been discovered in the system until now, a few ternaries have been found to exhibit intriguing physical phenomena, like complex long-range magnetic orderings and dense Kondo behaviors in $\text{Ce}_3\text{Rh}_3\text{Si}_2$ [4], CeRh_3Si_2 [5], Ce_2RhSi_3 [6] and CeRh_2Si [7]. In turn, the compounds CeRhSi_2 and $\text{Ce}_2\text{Rh}_3\text{Si}_5$ have been characterized as intermediate valence systems [8].

In this paper we report for the first time the results of our investigations on the low-temperature physical properties of five ternary compounds that form with ~25 and 33 at.% of cerium, namely $\text{CeRh}_{1.82}\text{Si}_{0.18}$ (at the edge of the homogeneity range of $\text{Ce}(\text{Rh}_{1-x}\text{Si}_x)_2$; MgCu_2 -type), $\text{Ce}_2\text{Rh}_{3.1}\text{Si}_{0.9}$ ($\text{Y}_2\text{Rh}_3\text{Ge}$ -type), $\text{CeRh}_3\text{Si}_{0.125}$ (CeRh_3 doped with Si; Cu_3Au -type), $\text{Ce}_4\text{Rh}_{12}\text{Si}$ (self-type) and $\text{Ce}_8\text{Rh}_{21.9}\text{Si}_{3.1}$ ($\text{Ce}_8\text{Pd}_{24}\text{Sb}$ -type).

2. Experimental details

Polycrystalline samples of $\text{CeRh}_{1.82}\text{Si}_{0.18}$, $\text{Ce}_2\text{Rh}_{3.1}\text{Si}_{0.9}$, $\text{CeRh}_3\text{Si}_{0.125}$, $\text{Ce}_4\text{Rh}_{12}\text{Si}$ and $\text{Ce}_8\text{Rh}_{21.9}\text{Si}_{3.1}$ were prepared by arc-melting high-purity elements (99.9 mass % Ce, 99.999 mass % Si and 99.99 mass % Rh) on a water-cooled copper hearth under argon atmosphere. To promote homogeneity, the melting was repeated several times with the button turned over between each melting. The weight losses were always less than 0.2 mass%. Subsequently, the alloys were vacuum-sealed in a quartz tube and annealed at 950 °C for two weeks. This heat treatment was finished with quenching in cold water.

* Corresponding author. Tel.: +48 71 34 350 21; fax: +48 71 34 410 19.
E-mail address: D.Kaczorowski@int.pan.wroc.pl (D. Kaczorowski).

Table 1
Crystallographic and EDX data of the Ce–Rh–Si samples.

Phase and homogeneity range Sample composition	Space group Prototype	Lattice parameters (nm)	EDX (at.%)		
			CCe	RRh	SSi
Ce(Rh _{1-x} Si _x) ₂ 0 ≤ x ≤ 0.1 CeRh _{1.82} Si _{0.18} (x = 0.09)	<i>Fd</i> $\bar{3}m$ MgCu ₂	a = 0.75265(1)	33.3	60.7	6.0
Ce ₂ Rh _{3+x} Si _{1-x} 0.08 ≤ x ≤ 0.17 Ce ₂ Rh _{3.1} Si _{0.9} (x = 0.1)	<i>R</i> $\bar{3}m$ Y ₂ Rh ₃ Ge	a = 0.55427(1) c = 1.18479(2)	33.1	52.2	14.7
Ce ₈ (Rh _{1-x} Si _x) ₂₄ Si 0.07 ≤ x ≤ 0.10 Ce ₈ Rh _{21.9} Si _{3.1} (x = 0.0875)	<i>Pm</i> $\bar{3}m$ Ce ₈ Pd ₂₄ Sb	a = 0.82676(2)	23.5	67.1	9.4
Ce ₄ (Rh _{1-x} Si _x) ₁₂ Si 0.00 ≤ x ≤ 0.03 Ce ₄ Rh ₁₂ Si (x = 0.0)	<i>Im</i> $\bar{3}m$ Ce ₄ Rh ₁₂ Si	a = 0.82072(3)	24.2	70.3	5.5
CeRh ₃ Si _{1-x} 0.81 ≤ x ≤ 1.00 CeRh ₃ Si _{0.125} (x = 0.875)	<i>Pm</i> $\bar{3}m$ Cu ₃ Au	a = 0.40655(2)	24.8	72.1	3.1

The products were examined by X-ray powder diffraction (XRD) and energy-dispersive X-ray analysis (EDX). The XRD data were collected at room temperature employing a STOE STADI P transmission diffractometer, equipped with a linear PSD (monochromatic CuK α_1 radiation with $\lambda = 1.54056 \text{ \AA}$; $10^\circ \leq 2\theta \leq 90^\circ$). Quantitative Rietveld refinements of the XRD patterns were performed employing the FULLPROF program [9]. The EDX studies were made using a Carl Zeiss LEO EVO 50XVP scanning electron microscope equipped with a Link EDX INCA Energy 450 system (Q-BSD detector).

Magnetic measurements were carried out over the temperature interval 1.71–400 K in magnetic fields up to 5 T employing a Quantum Design MPMS-5 SQUID magnetometer. The electrical resistivity was measured from 4.2 K to room temperature by a conventional four-probe dc technique implemented in a home-made setup. Electrical leads (copper wires) were attached to the bar-shaped specimens using silver-epoxy paste.

3. Results and discussion

3.1. Sample characterisation

The XRD and EDX analyses indicated single-phase character of the CeRh_{1.82}Si_{0.18}, Ce₈Rh_{21.9}Si_{3.1} and CeRh₃Si_{0.125} samples with no impurities. In turn, Ce₄Rh₁₂Si was present as a major phase in the relevant sample with a small amount (less than 0.5%) of cubic compound Ce₂Rh₁₅Si₇ as an impurity. In the case of Ce₂Rh_{3.1}Si_{0.9}, the electron probe microanalysis (EPMA) revealed significant inhomogeneity of the specimen: while bottom part of the sample had the proper composition, rather large amounts of CeRh₂ and CeRh₂Si impurity phases were detected on its upper part. For this very sample a slab of 1 mm thickness was prepared from the bottom part of the ingot for the physical property measurements. The lattice parameters and the phase compositions of all the samples investigated are summarized in Table 1. In general, they are in good agreement with the data reported in Ref. [1].

3.2. Physical properties

The magnetic behavior of the Ce–Rh–Si ternaries studied in this work is presented in the five panels of Fig. 1. For each compound the magnetic susceptibility is positive in the entire temperature range covered. Moreover, it is hardly temperature dependent over an extended temperature interval, and only at very low temperatures the $\chi_m(T)$ curves show some upturns. This behavior is characteristic of weak Pauli paramagnets, which contain impurities having a Curie–Weiss (CW) paramagnetic character. In the present case it implies that all the cerium ions in the studied compounds would be nominally tetravalent with nonmagnetic 4f⁰ configuration. In turn, the impurity might essentially contain Ce³⁺ ions (e.g., in form of cerium oxides located on grain boundaries), each of them characterized by the effective magnetic moment $\mu_{\text{eff}}^{\text{Ce}^{3+}} = 2.54 \mu_B$. For such a system the experimental data can be analyzed in terms of the function $\chi_m(T) = \chi_{\text{int}} + C_{\text{imp}}/(T - \theta_{\text{imp}})$, where a Curie–Weiss-

like term was added to the intrinsic temperature-independent susceptibility χ_{int} to account for the impurity contribution. The solid lines in Fig. 1 represent least-squares fits of this formula to the experimental data of CeRh_{1.82}Si_{0.18}, Ce₂Rh_{3.1}Si_{0.9}, CeRh₃Si_{0.125}, Ce₄Rh₁₂Si and Ce₈Rh_{21.9}Si_{3.1}, and the so-derived values of χ_{int} , C_{imp} and θ_{imp} are collected in Table 2. Attributing the spurious term to Ce³⁺ ions only, one may estimate their amount, n , from the obtained value of $C_{\text{imp}} = n(\mu_{\text{eff}}^{\text{Ce}^{3+}})^2/8$. These estimates are also given in Table 2. Clearly, the impurity content is very low in Ce₄Rh₁₂Si and Ce₈Rh_{21.9}Si_{3.1}, a bit larger in CeRh_{1.82}Si_{0.18} and CeRh₃Si_{0.125}, while it is relatively high in Ce₂Rh_{3.1}Si_{0.9}. This result well agrees with the EDX data collected for the samples studied. In line with this finding is also the magnitude of the magnetization reached at $T = 1.71 \text{ K}$ in a field of 5 T (see the insets to Fig. 1) that is much larger in Ce₂Rh_{3.1}Si_{0.9} in respect to that measured for the other specimens. Regardless this difference, for all the compounds $\sigma(H)$ has a similar shape, characteristic of paramagnetic systems. As apparent from Table 2, the intrinsic behavior of these samples is characterized by the Pauli susceptibility of the order of $10^{-4} \text{ emu}/(\text{mol Ce-atom})$, typical for nonmagnetic metals. Somewhat enhanced χ_{int} values were found for CeRh_{1.82}Si_{0.18} and Ce₂Rh_{3.1}Si_{0.9}, which seem indicate moderately strong electronic correlations (yet for the latter compound, any strong statement is hampered by the impurity contamination).

Fig. 2 presents the temperature variations of the electrical resistivity of the Ce–Rh–Si ternaries. These data reveal metallic nature of all these materials and corroborate their weakly magnetic character. In particular, the $\rho(T)$ curves measured for CeRh₃Si_{0.125}, Ce₄Rh₁₂Si and Ce₈Rh_{21.9}Si_{3.1} exhibit a behavior characteristic of nonmagnetic metals that can be described by the Bloch–Grüneisen–Mott (BGM) formula [10].

$$\rho(T) = \rho_0 + 4RT \left(\frac{T}{\Theta_R} \right)^4 \int_0^{\Theta_R/T} \frac{x^5 dx}{(e^x - 1)(1 - e^{-x})} - KT^3$$

where ρ_0 stands for the residual resistivity due to static defects in the crystal lattice, the second term describes the phonon contribution to the total resistivity (the parameter Θ_R is considered as a measure of the Debye temperature Θ_D), and the third one represents s–d interband scattering processes. As can be inferred from Fig. 2, the BGM expression provides very good approximations of the experimental $\rho(T)$ data of these three compounds, and the so-derived values of the transport parameters are collected in Table 2. Also the resistivity of CeRh_{1.82}Si_{0.18} can be represented by the BGM function, yet quality the least-squares fit is less good, especially close to room temperature, where $\rho(T)$ is markedly curved. Analysing the obtained parameters, it is worth noting that the ratio of the resistivity measured at room temperature to the residual resistivity is close to 1 (the only exception is Ce₄Rh₁₂Si), which can

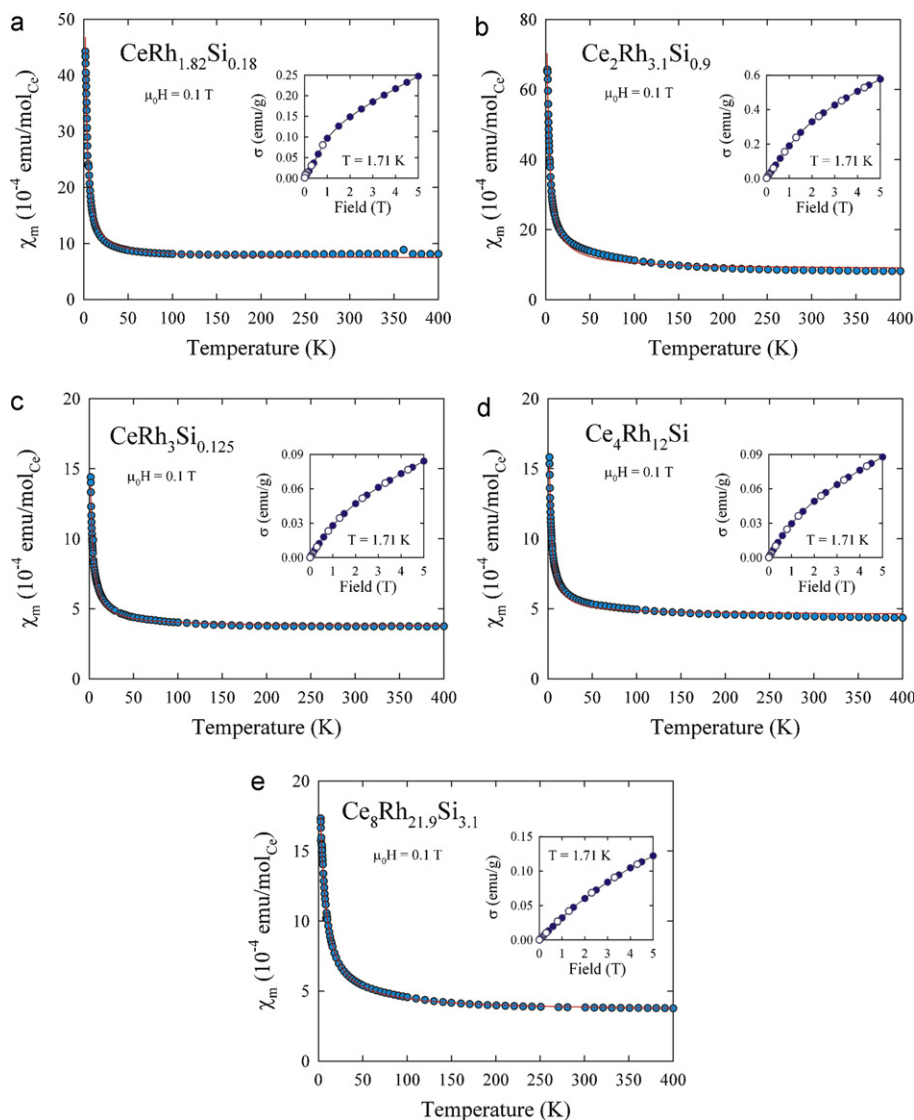


Fig. 1. Temperature dependencies of the molar magnetic susceptibility of (a) $\text{CeRh}_{1.82}\text{Si}_{0.18}$, (b) $\text{Ce}_2\text{Rh}_{3.1}\text{Si}_{0.9}$, (c) $\text{CeRh}_3\text{Si}_{0.125}$, (d) $\text{Ce}_4\text{Rh}_{12}\text{Si}$, and (e) $\text{Ce}_8\text{Rh}_{21.9}\text{Si}_{3.1}$, taken in a field of 0.1 T. The solid lines are the fits discussed in the text. The insets display the field variations of the magnetization measured at 1.71 K with increasing (full circles) and decreasing (open circles) the magnetic field strength.

be attributed to large degree of structural disorder inherent in all these ternaries [1] (here note that $\text{Ce}_4\text{Rh}_{12}\text{Si}$ exhibits full atomic order [1]). The scattering of conduction electrons on phonons, characterized by the values of Θ_R and R , appears similar in these compounds (an exception seems $\text{Ce}_4\text{Rh}_{12}\text{Si}$) and comparable to that in cerium-based intermetallics. In turn, the Mott contribution to the electrical conductivity is rather small (again except for the case of $\text{Ce}_4\text{Rh}_{12}\text{Si}$), while opposite signs of the parameter K derived

for these systems likely signal different curvatures of their electronic bands near the Fermi level.

As seen in Fig. 2, the temperature dependence of the electrical resistivity of $\text{Ce}_2\text{Rh}_{3.1}\text{Si}_{0.9}$ is entirely dissimilar to those found for the other Ce–Rh–Si silicides. Below about 50 K, $\rho(T)$ rapidly bends down and no saturation is observed down to the lowest temperatures measured. Such a behavior of the resistivity is typical for Ce-based systems with strong electronic correlations, and

Table 2
Magnetic and electrical characteristics of the Ce–Rh–Si samples.

Compound	$\text{CeRh}_{1.82}\text{Si}_{0.18}$	$\text{Ce}_2\text{Rh}_{3.1}\text{Si}_{0.9}$	$\text{Ce}_8\text{Rh}_{21.9}\text{Si}_{3.1}$	$\text{Ce}_4\text{Rh}_{12}\text{Si}$	$\text{CeRh}_3\text{Si}_{0.125}$
χ_{int} (10^{-4} emu/mol $_{\text{Ce}}$)	7.2	8.6	3.5	4.6	3.7
C_{imp} (10^{-3} emu/K mol $_{\text{Ce}}$)	9.5	18.8	9.7	2.8	2.9
n_{imp} (% per mol $_{\text{Ce}}$)	1.2	2.3	1.2	0.3	0.4
θ_{imp} (K)	−0.7	−1.3	−4.6	−0.9	−1.2
$\rho_{290\text{K}}$ ($\mu\Omega\text{ cm}$)	116.3	114.4	57.4	64.8	104.1
ρ_0 ($\mu\Omega\text{ cm}$)	106.8	–	42.0	20.8	90.3
$\text{RRR} = \rho_{290\text{K}}/\rho_0$	1.1	–	1.4	3.1	1.2
Θ_R (K)	213.3	–	212.5	147.6	183.2
R ($\mu\Omega\text{ cm/K}$)	0.039	–	0.053	0.164	0.046
K (10^{-8} $\mu\Omega\text{ cm/K}^3$)	−5.1	–	2.2	−11.3	3.3

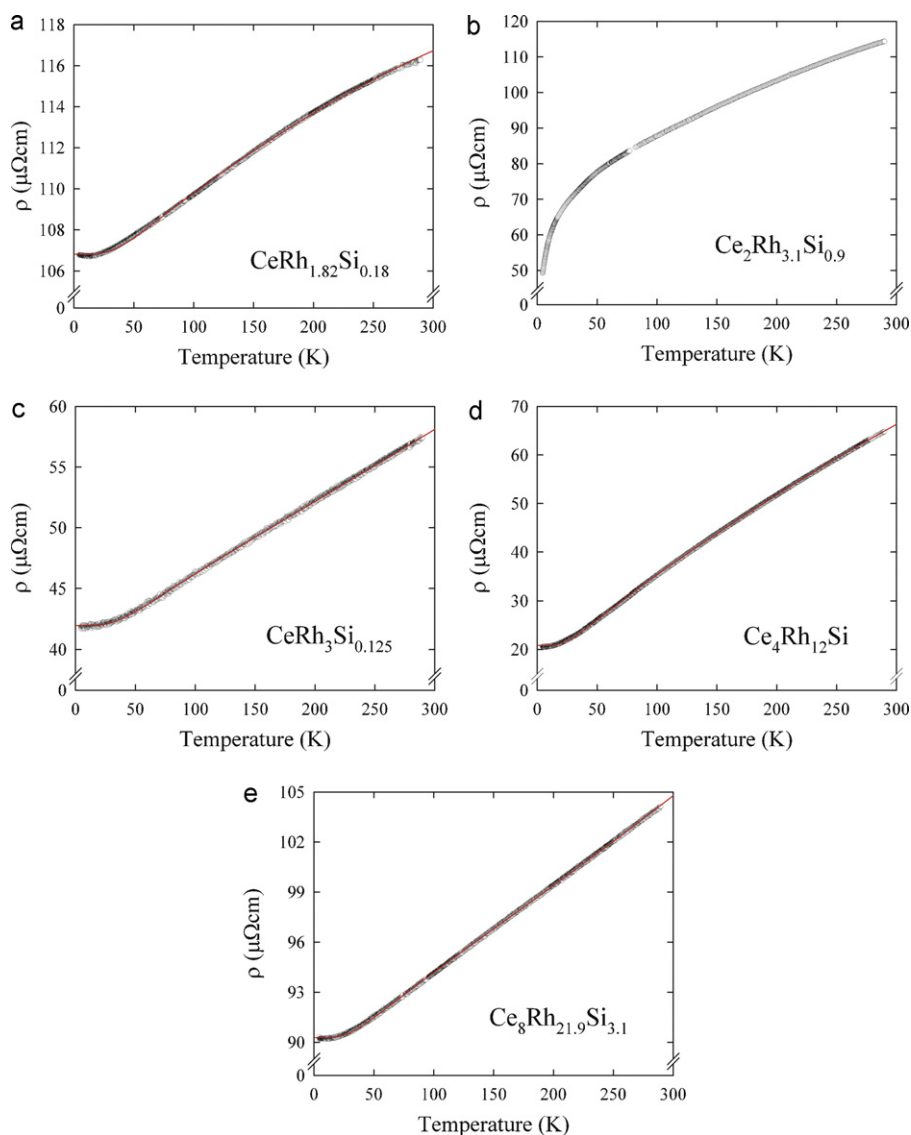


Fig. 2. Temperature dependencies of the electrical resistivity of (a) $\text{CeRh}_{1.82}\text{Si}_{0.18}$, (b) $\text{Ce}_2\text{Rh}_{3.1}\text{Si}_{0.9}$, (c) $\text{CeRh}_3\text{Si}_{0.125}$, (d) $\text{Ce}_4\text{Rh}_{12}\text{Si}$, and (e) $\text{Ce}_8\text{Rh}_{21.9}\text{Si}_{3.1}$. The solid lines represent the BGM fits discussed in the text.

seems compatible with the magnetic data of $\text{Ce}_2\text{Rh}_{3.1}\text{Si}_{0.9}$. Though the studied specimen contained some magnetic impurities (see above), it is very unlikely that the derived $\rho(T)$ variation was significantly affected by their presence, as the electronic transport in metals is known to be hardly sensitive to small amount of foreign phases. Therefore, the obtained results may be attributed to intrinsic behavior in $\text{Ce}_2\text{Rh}_{3.1}\text{Si}_{0.9}$ and hence hint at some instability in the valence state for the Ce ions. To further explore this conjecture, more detailed investigations of the transport and thermodynamic properties of the compound are required, performed at much lower temperatures and possibly on higher quality samples.

References

- [1] A. Lipatov, A. Gribov, A. Grytsiv, S. Safronov, P. Rogl, J. Rousnyak, Y. Seropegin, G. Giester, *J. Solid State Chem.* 183 (2010) 829.
- [2] (a) R. Movshovich, T. Graf, D. Mandrus, J.D. Thompson, J.L. Smith, Z. Fisk, *Phys. Rev. B* 53 (1996) 8241; (b) Y. Onuki, R. Settai, K. Sugiyama, T. Takeuchi, T.C. Kobayashi, Y. Haga, E. Yamamoto, *J. Phys. Soc. Jpn.* 73 (2004) 769.
- [3] N. Kimura, K. Ito, K. Saitoh, Y. Umeda, H. Aoki, T. Terashima, *Phys. Rev. Lett.* 95 (2005) 247004.
- [4] D. Kaczorowski, Y. Prots, U. Burkhardt, Y. Grin, *Intermetallics* 15 (2007) 225.
- [5] A.P. Pikul, D. Kaczorowski, Z. Gajek, J. Stjpień-Damm, A. Ślebarski, M. Werwiński, A. Szajek, *Phys. Rev. B* 81 (2010) 174408.
- [6] (a) M. Szwławska, D. Kaczorowski, A. Ślebarski, L. Gulay, J. Stjpień-Damm, *Phys. Rev. B* 79 (2009) 134435; (b) T. Nakano, K. Sengupta, S. Rayaprol, M. Hedo, Y. Uwatoko, E.V. Sampathkumaran, *J. Phys.: Condens. Matter.* 19 (2007) 326205.
- [7] D. Kaczorowski, A. Ślebarski, *Phys. Rev. B* 81 (2010) 214411.
- [8] (a) D. Kaczorowski, A.P. Pikul, U. Burkhardt, M. Schmidt, A. Ślebarski, A. Szajek, M. Werwiński, Y. Grin, *J. Phys.: Condens. Matter.* 22 (2010) 215601; (b) D.T. Adroja, B.D. Rainford, *J. Magn. Magn. Mater.* 119 (1993) 54; (c) C. Godart, C.V. Tomy, L.C. Gupta, R. Vijayaraghavan, *Solid State Commun.* 67 (1988) 677.
- [9] J. Rodriguez-Carvajal, "FULLPROF: a program for Rietveld refinement and pattern matching analysis", in abstracts of the Satellite Meeting on Powder Diffraction of the XV Congress of the IUCr, 1990, Toulouse, France, p. 127; T. Roisnel, and J. Rodriguez-Carvajal, in Materials Science Forum, Proceedings of the European Powder Diffraction Conference EPDIC7, 2000, p. 118.
- [10] N.F. Mott, H. Jones, *The Theory of the Properties of Metals and Alloys*, Oxford University Press, 1958.